Central line. (c) Connections of MMIs. (d) EAM covered by electrode and SiO2 mask. (e) Top view from microscope

5.4 Fabrication of all-optical switch

The process flow depends on the layer stacks of the grown substrate. In our case, different regrowth methods lead to different process. Moreover, fabrication with dry etching also differs greatly from that with wet etching.

In this section, we propose the fabrication process for the MZI-EAM switch whose substrate is grown by two-step butt joint technique.

5.4.1 Fabrication process for high mesa all-optical switches

As mentioned in Chapter II, we apply two-step regrowth for the forming of the passive region. So after the regrowth, p+-InGaAs whose carrier concentration is as high as 2e19, remains on top of the passive region, and brings significant internal loss. Therefore, it must be removed in the end. The detailed process flow is shown in Fig.5.4

At first, a 200nm SiO2 film is formed by magnetron sputtering. On top of it switch patterns are formed by contact photolithography with a Carl-Zuss mask aligner. Note that in this step, the active region in the grown sample should be adjusted to the EAM region in the mask. Here a thick and temperature resistant photo-resist (TSMR 8900) is used, as because previously used S1805 is too thin for the following dry etching and yields a tapered etching profile. The patterned photoresist is baked at 120°C for 15 minutes in an oven to strengthen its resistance against chemical etching. Then the samples are transferred into the chamber where the SiO2 film is etched by inductively coupled plasma (ICP) dry etcher with CHF3/Ar/O2 (1:9:0.3sccm gas flow ratio, source power of 200W, bias 25W, pressure 1Pa). After ashing off remaining photoresist, the SiO2 is formed (Fig5.4.1~4).

Subsequently, dry etching of InGaAs and InP material is done with the same ICP machine with the SiO2 mask, but with Cl2/Ar plasma. As mentioned in Chapter II???, the gas flow ratio is optimized to Cl2/Ar????. At an elevated temperature of 220°C, source 200W, bias 150W and 1Pa ambient, the

etching rate and etch selectivity of InP over SiO2 are 0.35μm/min and about 10, respectively; and the etch rate of InGaAs/InGaAlAs is 0.4 μm/min. The etching profile shows very little difference when we bonded the wafer to the chip carrier with silver paste or not. In our experiment, the etch depth is 2.3 μm after 8 min and 30 sec dry etching. The height is measured by a film height profiling machine (DEKTAK) and confirmed by the SEM photography. After the InP etching, the remaining SiO2 mask was etched away using the ICP O2 plasma ashing (Fig.5.4 5~6).

The second procedure is the contact opening for the electrode, which is shown in Fig.5.4.7~11. Firstly, a new 200nm thick SiO2 passivation layer is deposited with the magnetron sputtering machine. This layer defines the regions for electrical field in EAM and it also isolates the optical filed from the metalization layer in order to avoid high optical loss. Secondly, a very thin photoresist (AZ5200NJ) is coated on the top of the wafer, covering all the top of the waveguides and substrate, as shown in Fig.5.4.8. Then the photolithography is taken. The mask used in this lithography has wider openings and allows exposure of a region around the EAM. The exposure time is set to be 3.5 sec and the developing time, 20 sec. We find that after this step, part of the photoresist is removed. So the sample is transferred into the ICP chamber and O2 ashing is used 100sec to totally remove the remaining of the resist on top of the EAM and passive waveguide, meanwhile remain the photoresist in other region, as shown in Fig.5.4.9. Though it seems that the photolithography is not necessary, in fact, by only ICP O2 ashing, the photoresist on top of the EAM and passive waveguide can not be clearly removed without removing the photoresist in other region. Now, the SiO2 mask exposes on top of the waveguide and EAM, and is etched by either wet etching or dry etching. After that, all the remaining photoresist is removed by ICP O2 ashing for about 30 minutes.

The third procedure is the forming of the electrode on EAM. At first, a 200nm Ti and 300nm Au is deposited on the whole sample with an Electron Beam evaporation machine (ULVAC). The Ti layer is used as a transitional p-contact to achieve an ohmic contact behavior at the interface with highly p-doped InGaAs layer. The Au layer completes the electrode contact on account of its good electric conductivity. Then, the pattern of the p-contacts on the topside of the chip was defined in positive photoresist (AZ5200NJ) and the metal except for the electrode and its pads of EAM is wet chemically removed using appropriate etchant, followed by the wet etching of the exposed InGaAs contact layer by SH (1:1:5) for 30 second at 5oC. The chemical etchant for Au is KI+I2 aqueous

solution and for Ti is buffer hydrofluoric acid. Then the exposed SiO2 and the remaining photoresist are removed by ICP (Fig.5.4.12~18). After lapping the whole chip to a thickness of about 120μm, the n-type bottom side of the chip was also metalized using a plasma quick coating. Annealing of the metal contact is finally done in a rapid thermal annealer (RTA) at 400℃ for 30 seconds. The n-contact on the bottom side of the chip consist only of Au metal of a few hundreds nanometer.

According to the process mentioned above, an all-optical switch is fabricated, as shown in Fig.5.5.

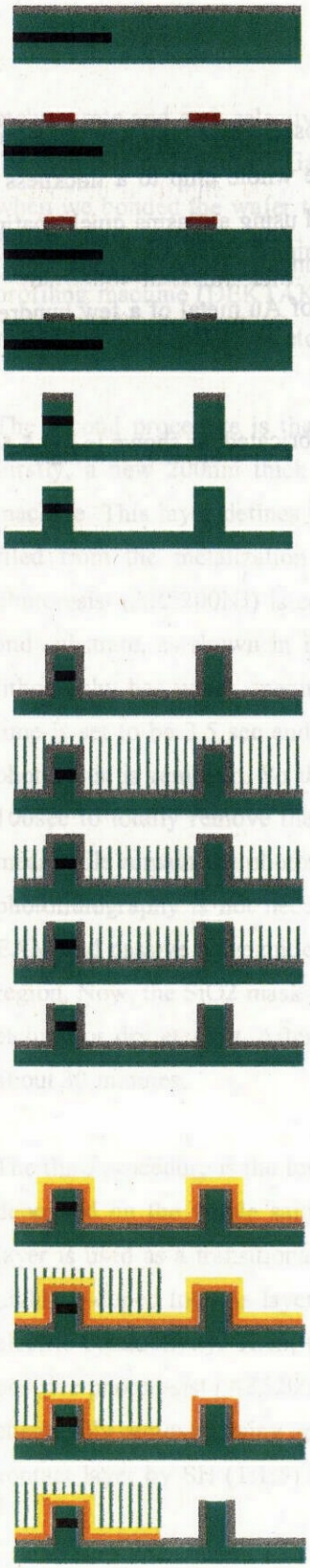

Procedure I: High mesa forming

1. SiO2 sputtering
2. Photoresist patterning by photolithography
3. SiO2 etching by ICP
4. Removal of the remaining photoresist by ICP (O2 ashing)
5. Forming of the high mesa structure by ICP
6. removal of the SiO2 mask by ICP

Procedure II: Contact opening

7. deposition of the SiO2 mask
8. Photoresist coating
9. thinning of the photoresist by ICP (O2 ashing)
10. removal of the SiO2 on top of the waveguide
11. Removal of the remaining photoresist

Procedure III: Electrode forming

12. Deposition of the Ti/Au electrode on the top side
13. Covering the active electrode by photoresist and removal of the remaining region by photolithography.
14. Etching the Au in passive region
15. Etching the Ti in passive region

Fig.5.4 Fabrication flows for the MZI-EAM high mesa all optical switch

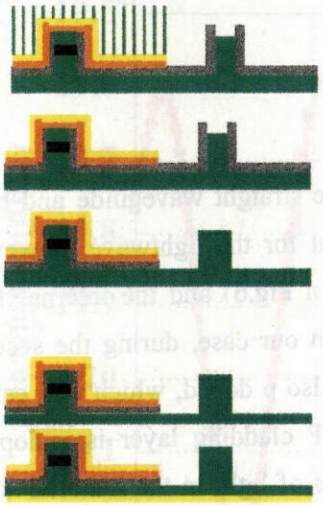

16. Etching of the InGaAs in passive region
17. Removal of the photoresist on top of the electrode in the active region
18. SiO2 etching by ICP or wet etching
19. Lapping the substrate
20. Electrode deposition on the back side.

Fig.5.4 Fabrication flows for the MZI-EAM high mesa all optical switch (continued)

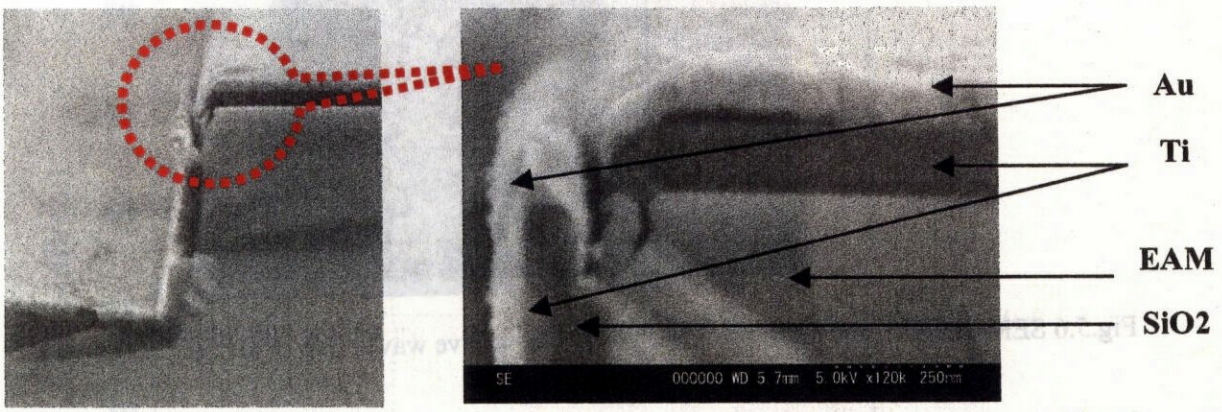

Fig.5.5 SEM images for the fabricated all-optical switch with high mesa. (SEM for whole device needed)

5.4.2 Fabrication process for ridge all-optical switches

The fabrication of the ridge all-optical switch is easier than that of high mesa one. The 1~6 steps in Fig.5.4 can be simplified to a standard photolithography and wet etching of the InGaAs/InP layers. For the electrode formation, both the contact opening and lift-off can be used.

5.5 Characterization of all-optical switch with high mesa

5.5.1 Passive waveguide loss measurement

Passive waveguide employed in the all-optical switch include straight waveguide and bent waveguide. The passive components are supposed transparent for the lightwave, however, due to the roughness on the waveguide sidewall (as shown in Fig.6) and the internal free carrier absorption, the propagation loss is large. Especially, in our case, during the second regrowth, the InP cladding layer in the passive waveguide is also p doped, which will cause additional loss compared to one-step regrowth where the InP cladding layer is undoped. Therefore, it is very important to confirm the propagation loss of light in the material with which we fabricate our devices.

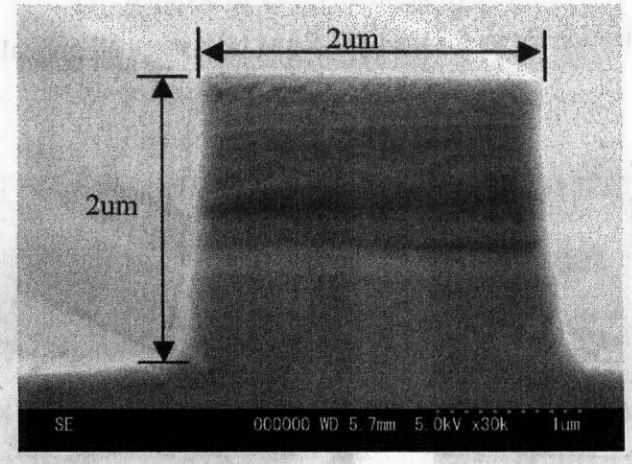

Fig.5.6 SEM image of the cross section view of the passive waveguide with high mesa.

In order to measure the loss in the passive waveguide, we cut a straight line with 600 um length from the all-optical switch. The Fabry-Perot method is used. The measurement result is shown in Fig.5.7. Fig. 5.7 (a) gives the raw data from the Fabry-Perot Etalon method, and Fig. (b) is obtained by using the expression (3.4)

$$\alpha = -\frac{1}{l}\ln\left(\frac{1}{r_1 r_2}\cdot\frac{\sqrt{H}-1}{\sqrt{H}+1}\right)$$

by assuming that r_1r_2=0.3. Seen from Fig.5.??(b), we find that the absorption of TE mode and TM mode are almost the same, 45dB/cm. This shows that the high mesa structure has the potential for polarization independence operation.(ref???). The typical value in our lab for 2um waveguide with high mesa etched by ICP is 40dB/cm. We think the additional loss in our case arise from the p-doping in the waveguide region.

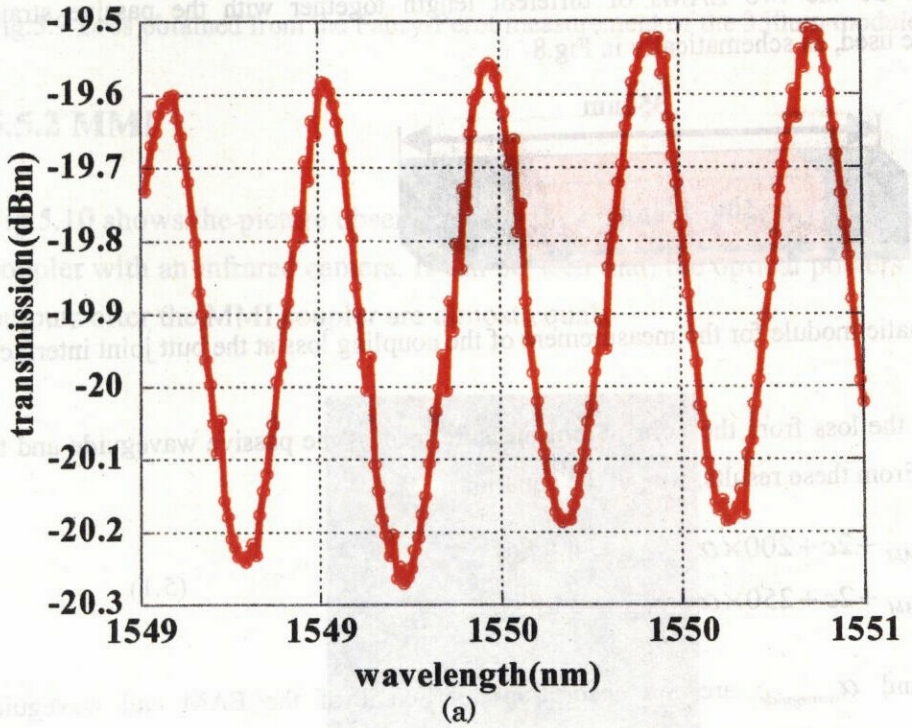

(a)

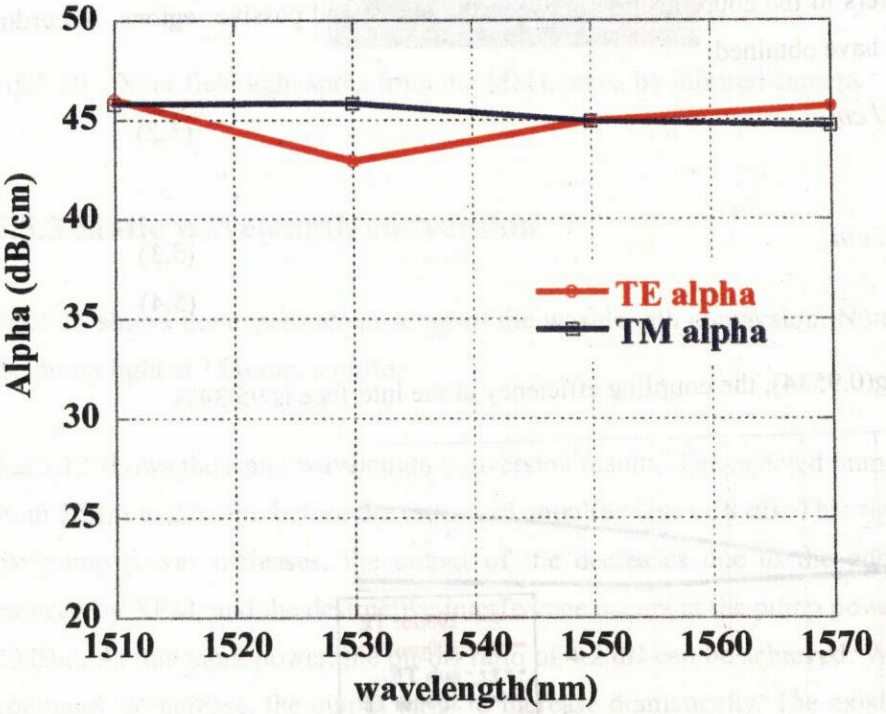

(b)

Fig.5.7 Loss measurement of the passive waveguide with high mesa etched by ICP. (a) data from the Fabry-Perot measurement. (b) absorption coefficient for both TE and TM mode.

For in the all optical switch, the EAM is only about 150 um, we can not cleave it for the measurement. So the two EAMs of different length together with the passive straight waveguide are used, as schematically in Fig.8

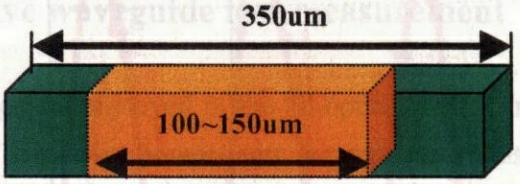

Fig.5.8 Schematic module for the measurement of the coupling loss at the butt joint interface.

Fig.5.9 shows the loss from the Fabry-Perot measurement of the passive waveguide and the joint module. From these results, we get the equation

$$\begin{cases} 150\times\alpha_{EAM}+2c+200\times\alpha_{waveguide}=4.8424 \\ 100\times\alpha_{EAM}+2c+250\times\alpha_{waveguide}=3.887 \end{cases} \quad (5.1)$$

where α_{EAM} and $\alpha_{waveguide}$ are the absorption coefficient of the EAM and waveguide respectively, c refers to the coupling loss between the active and passive regions. According to Fig.5.7 (b), we have obtained

$$\alpha_{waveguide}=45dB/cm \quad (5.2)$$

So

$$\alpha_{EAM}=236.1dB/cm \quad (5.3)$$

$$c=0.21\text{dB}. \quad (5.4)$$

For –0.21dB=10 lg(0.9534), the coupling efficiency at the interface is 95.34%.

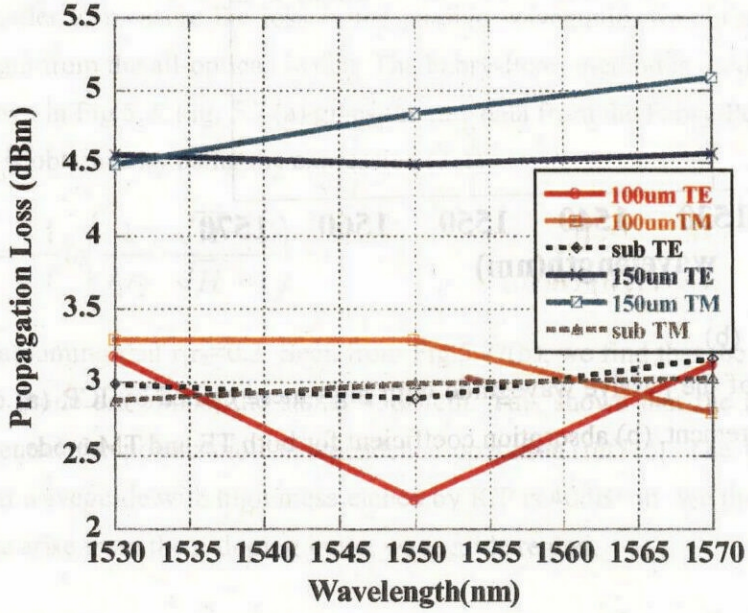

Fig.5.9 Loss obtained from the Fabry-Perot measurement of the 350um module.

5.5.2 MMI

Fig.5.10 shows the picture observed from the output facet of the fabricated MMI coupler with an infrared camera. It can be seen that, the optical powers from the two outputs after the MMI coupler are almost equal.

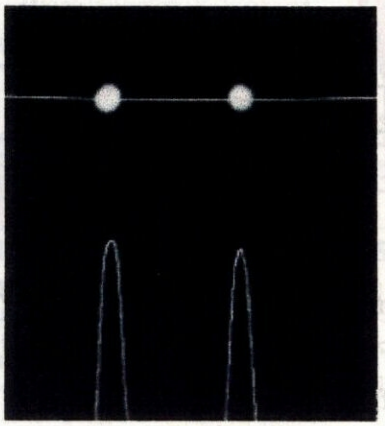

Fig.5.10 Near field light spots from the MMI, taken by infrared camera.

5.5.3 Static wavelength conversion

Fig.5.11 shows the experimental setup of the wavelength conversion. Note that in this setup, the pump light at 1540nm is pulse.

Fig.5.12 shows the static wavelength conversion results. The injected pump power is changes from 2dBm to 22dBm, before the estimated coupling loss of 8 dB. This figure indicates when the pump power increases, the output of the decreases due to the additional phase shift induced by XPM, and the destructive interference occurs at the pump power of approximately 20dBm. At this input power, the on-off ratio of 4.2 dB can be achieved. When the pump light continues to increase, the output turns to increase dramatically. The existence of the turning point is a convictive evidence of the phase modulation. It verified that the validity of the proposal of all optical switches with EAM as the optical phase modulator.

Fig.5.13 shows the spectra of the outputs after the all-optical switch in the optical spectrum analyzer (OSA). From Fig.5.13 (a), it can been seen that the 1540nm pump light is effectively filtered out, so the output is only from the 1550nm probe light. Fig.5.13 (b) is the enlarged

view of the circle part in Fig.5.13 (a). We can see that the peak of the output of 1550nm light becomes smaller under the injection of the pump light. This matches well with the results shown in Fig.5.12.

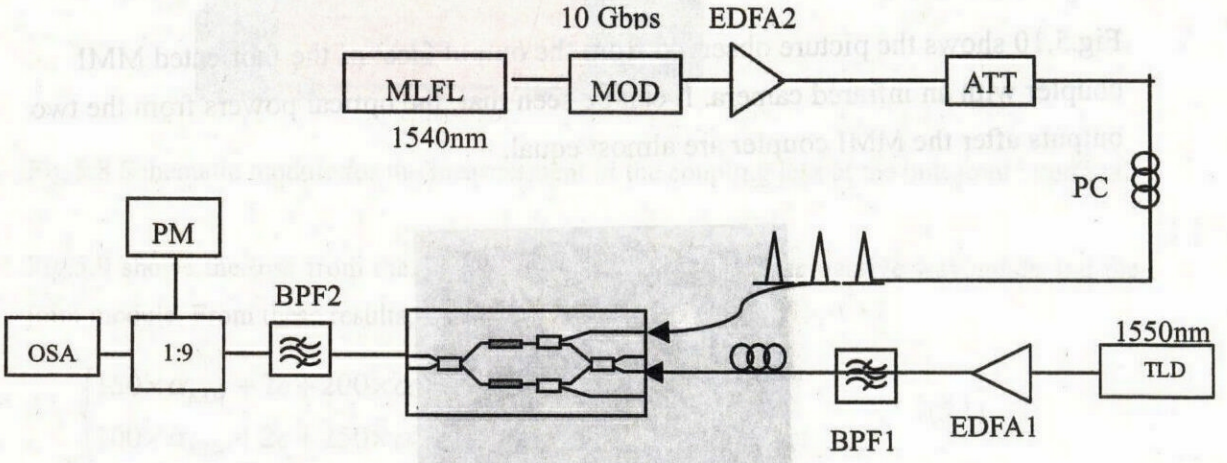

Fig.5.11 Schematic experiment setup for wavelength conversion. TLD: tunable laser diode, PC: polarization controller, BPF: band-pass filter, PM: power meter, OSA: optical spectrum analyzer, MLFL: mode-locked fiber laser, MOD: electrooptical modulator, EDFA: Er-doped fiber amplifier.

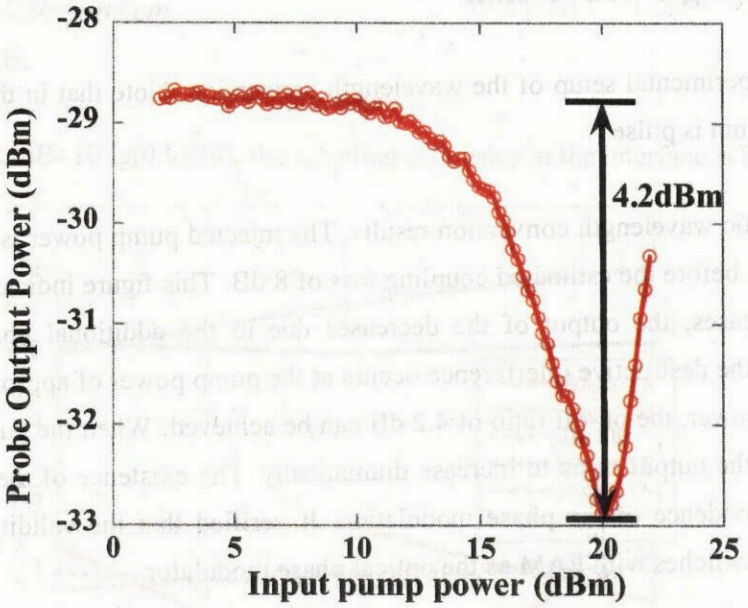

Fig.5.12 Static wavelength conversion results. The pump light is at 1540nm and the probe light is at 1550nm.

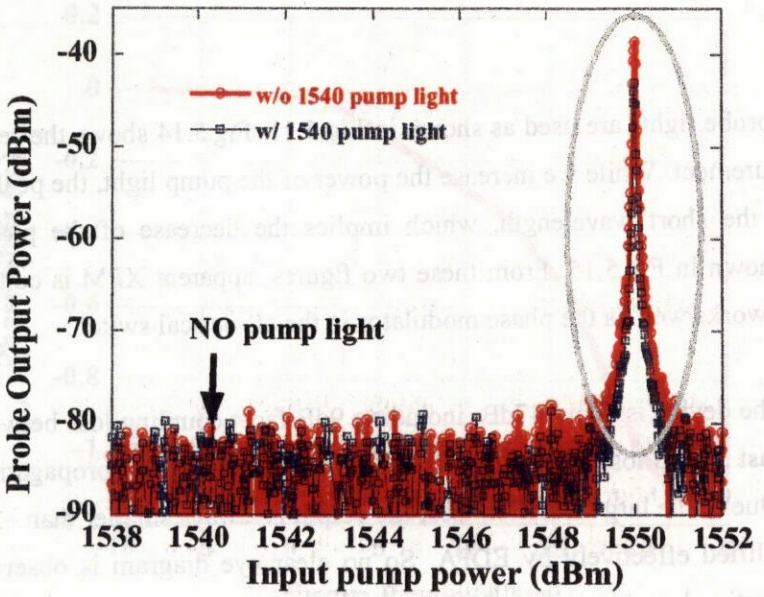

(a)

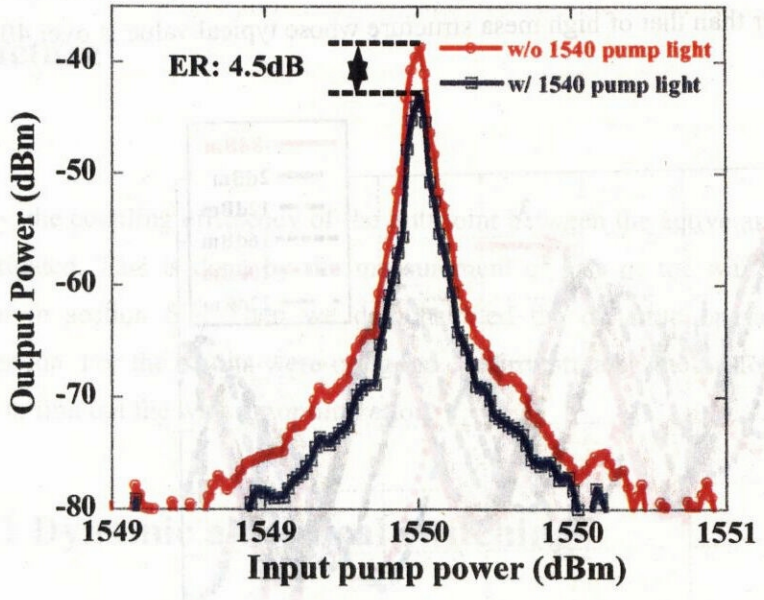

(b)

Fig.5.13 Spectra of the outputs after the all-optical switch with high mesa in the optical spectrum analyzer (OSA). The red line denotes the spectrum with the 1540nm pump light injected into the switch, and the blue line denotes that without pump light. The wavelength in (a) covers both 1540nm and 1550nm. (b) is the zoom of the circled part in (a).